Arabian Journal for Science and Engineering (2018) 43:3103–3114
https://doi.org/10.1007/s13369-018-3151-0

RESEARCH ARTICLE - ELECTRICAL ENGINEERING

Design and Analysis of Tilt Integral Derivative Controller for Frequency Control in an Islanded Microgrid: A Novel Hybrid Dragonfly and Pattern Search Algorithm Approach

Rajendra Kumar Khadanga[1] · Sasmita Padhy[2] · Sidhartha Panda[2] · Amit Kumar[3]

Received: 30 September 2017 / Accepted: 8 February 2018 / Published online: 26 February 2018

Abstract
In this research work, a maiden approach is made for the frequency control in an islanded AC microgrid (MG). A MG can be formed by combining the different sources like renewable energy source, wind power generation and the solar energy generation. Variation in any of the source influences the MG frequency, and thus, the frequency control issue for MG is always a challenge for the researcher industry. In light of these difficulties, this paper considers a tilt integral derivative (TID) controller for the secondary frequency control of the islanded MGs and a novel hybrid dragonfly algorithm and pattern search (hDF-PS) algorithm is used to tune the controller parameters. In the proposed control conspire, some sources like microturbine, diesel engine generator and fuel cell are used which balance the load and power can demand of the MG. The novel hybrid controller is inspected on a MG test system, and the robustness and execution are assessed by considering different disturbances and parametric variations. In order to show the effectiveness of the proposed hybrid algorithm-based TID controller, it is being compared with some conventional controllers like integral, proportional integral and proportional integral derivative-based controller. It can be demonstrated that the proposed hDF-PS-based TID controller approach (because of considering organized/parametric instabilities) gives preferably better execution over the other control techniques.

Keywords Microgrid (MG) · Renewal energy sources · Tilt integral derivative (TID) controller · Hybrid dragonfly algorithm and pattern search (hDF-PS) algorithm

List of symbols

BES	Battery energy storage
D	Damping coefficient
DEG	Diesel engine generator
DER	Distributed energy resource
DG	Distributed generator
f	Frequency deviation
FES	Flywheel energy storage
FC	Fuel cell
LFT	Linear fractional transformation
M	Inertia constant
MG	Microgrid
MGCC	MG central controller
MT	Microturbine
NP, NS	Nominal performance and nominal stability
PV	Photovoltaic panel
P_{DEG}	DEG output power change
P_{MT}	MT output power change
P_{FC}	FC output power change
P_{PV}	PV output power change
P_{BES}	BES output power change
P_{FES}	FES output power change
P_{ϕ}	Solar radiation power change
P_{Wind}	Wind power change
P_{L}	Load power change
P	Real power unbalance

✉ Rajendra Kumar Khadanga
rajendra697@gmail.com

Sasmita Padhy
sasmita_padhy@hotmail.com

Sidhartha Panda
panda_sidhartha@rediffmail.com

Amit Kumar
amitsynergy2007@gmail.com

[1] Department of Electrical Engineering, NIST, Berhampur, India

[2] Department of Electrical Engineering, VSSUT, Burla, India

[3] Department of Electrical Engineering, NIT Rourkela, Rourkela, India

RES	Renewable energy source
RP, RS	Robust performance and robust stability
Δ	Uncertainty block
T_{DEG}	DEG time constant
T_{MT}	MT time constant
T_{FC}	FC time constant
T_{WTG}, T_{PV}	WTG and PV time constants
T_{BES}, T_{FES}	BES and FES system time constants
WTG	Wind turbine generator

1 Introduction

In the recent years, development of remote off-grid MGs helps in supplying electrical energy for the rural areas where the conventional way of supplying energy from a grid is too costly. Therefore, numerous MGs are introduced for supplying electricity to those areas.

A MG can be operated in two modes: islanded mode and the grid connected mode. Out of these two, the islanded mode of operation of a MG is more troublesome compared to the grid connected mode. This is because in the grid connected mode the regulation of voltage/frequency is supported by the main supply, whereas in the islanded mode of operation the wind power and solar irradiation resources are used to compensate the load variations [1]. The factors responsible for the real operation of a MG are nonlinear structure, dynamic complexity, instabilities and discontinuous nature of DER. If the power mismatch between the load and generator occurs, then it creates a deviation in frequency and voltage from its original value which leads to MG blackout. Hence, the optimized controller design technique is useful to accomplish the stability of the system within the sight of different load deviation and some environmental condition with in MGs [2].

The distributed assets and renewal sources like DEG, WTG, FC, BES, PV, FC and FES systems assume an indispensable part for the MG structure. For choosing DERs for an islanded MG system, the primary elements are the environmental and economic constraints. The power generated by the renewal sources like WTG and the PV mainly relies on the climate condition; thus, they cannot be used as the secondary frequency control [3]. The function of MT and DEG sources is to supply a part of electrical energy to the demand side which can repay the inadequacy in electrical energy. However, these are associated with some disadvantages like slow response time, inability to handle MG control during the sudden changes in load and power demand etc. Therefore, in order to archive a rapidly compensation, coordination of MT or DEG with some other energy storage elements is highly required [4].

The primary aim of this paper is to propose a robust frequency control for a MG in the secondary regulation loop. The optimal requirement of the MG can be achieved by adjusting the set points, and the process is carried out by the secondary frequency control [5]. For the secondary control in MG, two fundamental structures are considered; first one is the centralized, and the second one is the decentralized structures. The centralized structure depends on the working of microgrid centralized controller (MGCC), and the decentralized plan permits the association of the different units inside the MG [6,7]. For the islanded operation of MGs, a centralized structure is preferred which is considered in our proposed study, while the decentralized approach is preferred for the grid-connected MGs [6]. The application of different types of robust controllers on the MG frameworks is given in the literatures [7–9]. Etemadi et al. [7] presented a decentralized control for the islanded MG. Han et al. proposed a μ-based controller for the frequency regulation in a MG. This μ-combination controller was outlined by a D-K iteration method. Kahrobaeian et al. [9] demonstrated some complex works on robust control of a μ-synthesis controller.

The secondary control of MG is described in the literature [10–13]. The applications of different methods for the frequency control of MGs are provided in [5,14,15]. Guerrero et al. presented the application of Hopfield fuzzy neural network algorithm and the combined particle swarm optimization (PSO) with fuzzy logic method for the regulation of frequency deviations. In [14], the proportional–integral–derivative was used to improve the frequency control execution and strength within the sight of instabilities and the PSO-based mixed H2/H∞ was proposed to tune the parameters of the controller. The application of fuzzy-based proportional–integral–derivative (PI) controller for the stability operation of MG system along with MT, FC and ES [15]. Further utilizations of some established control techniques are also described in MG control.

In the conventional control techniques, the effective exchange off states between NPs and RPs are very difficult to accomplish. However, the robust control techniques (because of possibility of uncertainties definition in the control synthesis strategy) fulfill this objective effectively. As the linear control methods have some physical limitations and uncertainties, these provide a successful control for the dynamical system. However, many of the control strategies propose a complex controller for which the order remains same for both the controller and the system [16]. Therefore the small size of MGs, compared to the conventional large-scale power systems, motivates to use these powerful synthesis methodologies for the MGs control problems.

This paper utilizes a TID controller which has been connected for the frequency control issue of microgrid. In the proposed (TID) controller, the corresponding part of PID controller is supplanted with a tilted component having a transfer function $s^{-1/n}$. The subsequent transfer function of the TID controller all the more nearly approximates an

optimal transfer function, there by accomplishing enhanced feedback controller. The subsidiary method of PID controller however enhances strength of the stability of the system and expands speed of the controller reaction, produces irrational size control input to the plant. The optimal estimation of TID controller parameters is acquired by minimizing the performance index, ITAE-integral of time-weighted absolute error. Additionally, comparison between the dynamic reaction acquired from integral (I) controller, proportional integral (PI) controller and proportional integral derivative (PID) controller has been displayed in this paper. For a uniform relative analysis, each one of the controllers is optimized utilizing same optimization technique, i.e., hybrid dragonfly and pattern search algorithm, and their execution has been analyzed in light of system response. Therefore, by enhancing the system stability and response, the TID controller indicates preferable better execution over I, PI and PID controller in microgrid issue.

Whatever is left of this paper is sorted out as takes after. Section 2 portrays the modeling of microgrid, and Sect. 3 represents the state-space dynamical modeling of MG. The modeling of the proposed tilt integral derivative controller strategy with a specific end goal is provided in Sect. 4. Section 5 demonstrates the description of the proposed hybrid dragonfly and pattern search algorithms. The time-domain performance of hybrid DF–PS-based tilt integral derivative controller with respect to the MG secondary control is shown in Sect. 6. At long last, the conclusion of the proposed research is presented in Sect. 7.

2 Modeling of Microgrid

A simplified setup for an islanded AC MG is shown in Fig. 1. It consists of DEG, WTG, PV, MT, FC and some energy storage devices like BES along with some AC loads. As shown in Fig. 1, in MG the power electronic-based devices are used for synchronizing the operations of sources like DEG and WTG and connecting the distributed resources to the ac bus by rectifying the dc voltages into ac sources. A converter is additionally considered for the BES system, which operates either in charging (ac to dc) or discharging (dc to ac) mode. Thus, the total generated power by the distributed resources, which is used to supply the demand side, is:

$$P_{\text{Load}} = P_{\text{DEG}} + P_{\text{MT}} + P_{\text{WTG}} + P_{\text{PV}} + P_{\text{FC}} \pm P_{\text{BES}} \pm P_{\text{FES}} \tag{1}$$

The RESs like WTGs and PVs are not used for the secondary control of the MGs because of their dependency on the environmental conditions. Therefore, the DEG, FC and MT are used for the secondary frequency control problem in this. In the frequency control loop, the power variation in WTG, PV and load is supplied by the power variation in MT and DEG. The change in MG frequency regulation can be expressed as:

$$\Delta P_{\text{Load}} + \Delta P_{\text{DEG}} + \Delta P_{\text{MT}} + \Delta P_{\text{FC}} + P_{\text{PV}} + \cdots \Delta P_{\text{WTG}} \pm \Delta P_{\text{BES}} \pm P_{\text{FES}} = 0 \tag{2}$$

Some of the simplified versions of the dynamical models for the DG units are shown in the literatures [11,17], and for many of the distributed sources, the order of the dynamical frequency reaction models is very high. In this paper, a low-order dynamic model is considered for frequency control issue of the MG due to simplicity [11]. Figure 2 demonstrates the dynamical frequency model for a MG, and the different system parameters are spoken in Table 1.

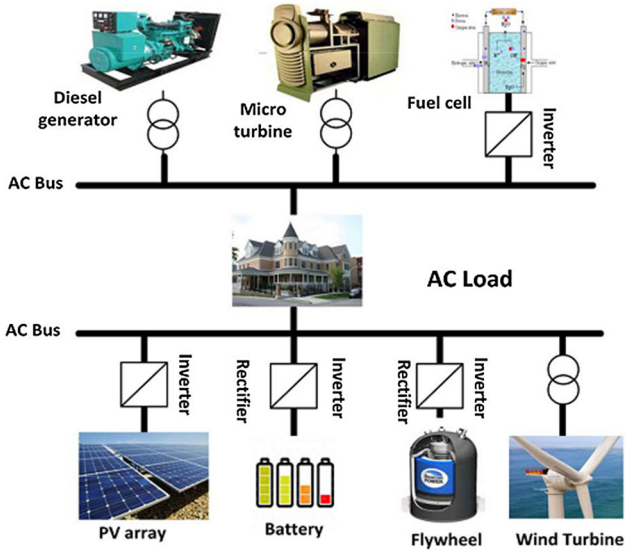

Fig. 1 Simplified schematic of an islanded MG

Table 1 Parameters of frequency response model

Parameters	Value	Parameters	Value
D (pu/HZ)	0.012	T_{DEG} (s)	2
M (pu/s)	0.2	T_{MT} (s)	2
T_{FC} (S)	4	T_{WTG} (s)	1.5
T_{BESS} (s)	0.1	T_{PV} (s)	1.8
T_{FESS} (s)	0.1		

3 State-Space Dynamic Model

In order to synthesize a MG, the linearized state-space model is essential. Utilizing the state variables (Eqs. 3–6), the state-space acknowledgment in the linearized form for the MG system (Fig. 2) can be obtained as [17].

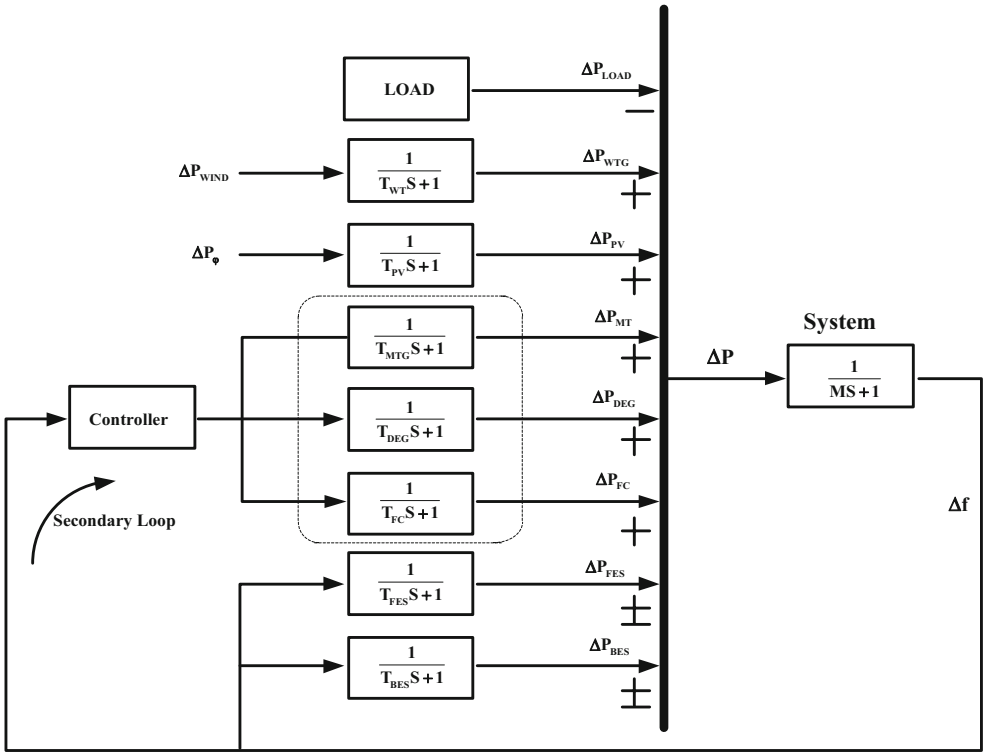

Fig. 2 MG dynamical frequency response model

$$\dot{x} = \mathrm{A}x + B_1 w + B_2 u$$
$$Y = C\dot{x} \tag{3}$$

where

$$x^{\mathrm{T}} = [\Delta P_{\mathrm{WTG}} \quad \Delta P_{\mathrm{PV}} \quad \Delta P_{\mathrm{DEG}} \Delta P_{\mathrm{FC}} \quad \Delta P_{\mathrm{MT}} \quad \Delta P_{\mathrm{BES}} \quad \Delta P_{\mathrm{FES}} \quad \Delta f] \tag{4}$$
$$w^{\mathrm{T}} = [\Delta P_{\mathrm{Wind}} \quad \Delta P_{P\varphi} \quad \Delta P_{\mathrm{Load}}] \tag{5}$$
$$y = \Delta f \tag{6}$$

where u represents the input control signal, ΔP_{Wind}, ΔP_{ϕ} and ΔP_{Load} are taken as the disturbance signals for the MG along with M and D as the uncertain parameters. Some complicated and nonlinear models for MG are also demonstrated in [3,10,18,19].

4 Tilt Integral Derivative Controller Design

The TID controller is basically a tuneable compensator having K_{P}, K_{I} and K_{D} as three control parameters with a tuning parameter as n. The structure of TID is like PID, aside from the proportional behavior is supplanted by a tilted proportional behavior having transfer function $1/\mathrm{S}^{1/n}$ or $\mathrm{s}^{-1/n}$. This transfer function block is referred as a 'Tilt' compensator, and the complete structure of compensator is referred as a tilt-integral-derivative (TID) compensator or controller. It has superior properties of maintaining system response stable under disturbance, during parameter variations, and it is easily tuned as well [20]. The tilted behavior gives a feedback gain as a component of frequency which is tilted regarding the pick gain/frequency of ordinary compensator. Thus, the whole compensator is alluded to as tilt-integral-derivative (TID) compensator. A piece chart portrayal of the TID control is shown in Fig. 3. The mathematical expression for the above discussion can be explained as:

$$U_{\mathrm{TID}} = G_{\mathrm{TID}}(s, \theta)\, E_{\mathrm{TID}}(s)$$
$$E_{\mathrm{TID}} = R_{\mathrm{TID}}(s, \theta) - Y_{\mathrm{TID}}(s)$$

where $G_{\mathrm{TID}}(s, \theta)$ the transfer is function of the TID controller in complex variable $S \in C$ and parameterized by $\theta \in R^4$. The mathematical description of transfer function $G_{\mathrm{TID}}(s, \theta)$ is:

$$G_{\mathrm{TID}}(s, \theta) = \frac{K_T}{s^{\frac{1}{n}}} + \frac{K_I}{s} + K_S$$

where $\theta^{\mathrm{T}} = [K_T \quad K_I \quad K_D \quad n]$

And $\theta \in R^4$, here θ is a vector of four control parameters K_{P}, K_{I}, K_{D} and n where $n \in R$ and $n \neq 0$. The range of n is ideally in the vicinity of 1 and 10. TID control offers high level of flexibility in control parameters and liable to have

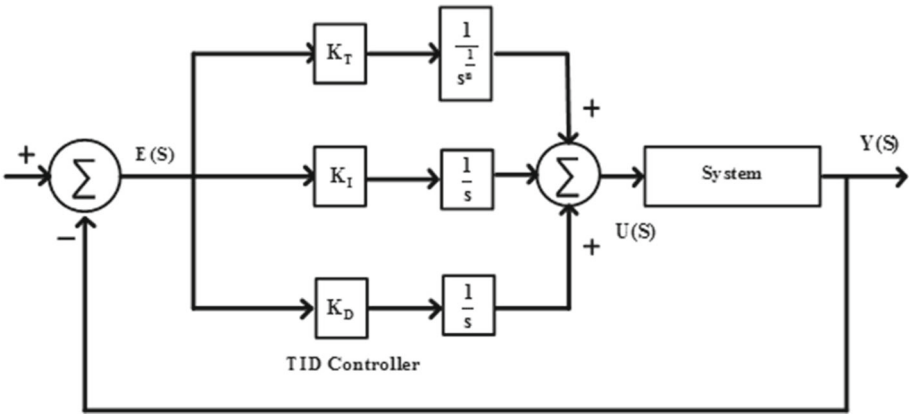

Fig. 3 Structure of TID controller in a closed loop system

predominant properties like simpler tuning, higher rejection ratio and smaller effects of plant parameter minor departure from closed loop response.

In the present configuration of a nature inspired optimization technique-based controller, initially the fitness function is formulated. The fitness function is used to optimize and tune the controller parameters. For any system, the typical parameters in the time domain for performance study are of maximum overshoot, rise time, settling time and steady-state error. In the field of controller design, usually four types of performance criteria are considered. They are integral of absolute error (IAE), integral of squared error (ISE), integral of time multiplied squared error (ITSE) and integral of time multiplied absolute error (ITAE) [21,22]. ISE error criterion aggregates the square of the error over the time; hence, huge errors are amended as compared to smaller error value.

ITSE introduces the sum of time multiplied square error, and IAE criterion only signifies the absolute error. Thus, these error criteria are not regularly utilized as objective function as a part of controller design [23]. ITAE objective function incorporates the integration of the absolute error multiplied by the time; therefore, it introduces errors which actually exist and are usually required for the controller design [24,25]. Thus, for MG operation the ITAE is the best objective function in all aspects and consequently used in the work.

The ITAE-based fitness function for the said MG can be written as:

$$J = \text{ITAE} = \int_0^{t_{\text{sim}}} |\Delta F| \cdot t \cdot \mathrm{d}t \tag{7}$$

where ΔF the change in the frequency deviation of the MG and t_{sim} the simulation time.

Here, the limits to the controller parameters are considered as constraints, while optimizing the controller gains. Therefore, the consider problem may be formulated as a optimization problem as described below:

$$\text{Minimize } \mathbf{J} \tag{8}$$

Subject to

$$\begin{aligned} K_{\text{P min}} &\le K_P \le K_{\text{P max}} \\ K_{\text{I}_{\text{min}}} &\le K_I \le K_{\text{I}_{\text{max}}} \\ K_{\text{D}_{\text{min}}} &\le K_D \le K_{\text{D}_{\text{max}}} \\ n_{\text{min}} &\le n \le n_{\text{max}} \end{aligned} \tag{9}$$

where J is the fitness function and $K_{X_{\text{min}}}$ and $K_{X_{\text{max}}}$ are the minimum and maximum limits of the controller gain parameters.

5 Hybrid Dragonfly Algorithm Pattern Search Algorithm (hDF-PS)

5.1 Dragonfly Algorithm

Reynolds states that the swarm behavior always follows three fundamental principles [26]:

(A) Separation: This refers to the avoidance of static collision of any individuals from the rest in a prescribed region.
(B) Alignment: This coordinates speed of the individual element to that of others in a prescribed region.
(C) Cohesion: This alludes to the propensity of each elements toward the others in a prescribed range.

'Survival of fittest' is the fundamental goal for any swarm-based algorithm; thus, each individual in a region ought to be pulled toward the source of food and diverted the enemies. By considering the facts discussed, a conclusion can be made that five variables are responsible for updating the individual element in swarms.

The separations is ascertained as takes after:

$$S_i = -\sum_{\text{j}=1}^{\text{N}} x - x_{\text{j}} \tag{10}$$

where X represents the current individual position, X_j represents the position of jth individual and N is the total neighboring individuals. The calculation of alignment is done as:

$$A_i = \frac{\sum_{j=1}^{N} V_j}{N} \tag{11}$$

where X_j represents the velocity of jth individual.

To calculate the cohesion, the following expression is used:

$$C_i = \frac{\sum_{j=1}^{N} x_j}{N} - X \tag{12}$$

The force of attraction near to a food source can be calculated as:

$$F_i = X^+ - X \tag{13}$$

where X^+ represents the food source's position, X^- is the enemy's position.

An enemy's distraction is calculated as:

$$E_i = X^- + X \tag{14}$$

Therefore, it is assumed that the conduction of dragonflies is thought to be the blend of five patterns. In order to upgrade each dragonfly position with in a prescribed space, two factors such as 'step (ΔX)' and 'position (X)' are considered. Out of these two factors, the step vector is the analogy of the velocity vector (in PSO), and thus, the proposed DA algorithm is created in view of the PSO algorithm. The movement of dragonflies is mainly influenced by the position of the step vector which is formulated as:

$$\Delta X_{t+1} = (sS_i + aA_i + cC_i + fF_i + eE_i) + w\Delta X_t \tag{15}$$

where s represents the weight separation, S_i shows the ith individual separation, a weight alignment factor, A ith individual alignment, C represents cohesion weight, C_i represents the ith individual cohesion, F represents the food factor, F_i shows the ith individual food source, E represents the enemy factor, E_i represents ith individual enemy position, w represents inertia weight, t number of counts of the iteration. Then, the position vector can be obtained as:

$$X_{t+1} = X_t + \Delta X_{t+1} \tag{16}$$

A balance between the explorative and exploitative can be accomplished during the optimization process by utilizing the above discussed factors. In the DF algorithm, neighbors of each dragonfly play a vital role, so each dragonfly is free to move with in a prescribed boundary. As talked about in the past subsection, two types of swarms (static and dynamic) are responsible for the behavior of dragonflies. The dragonflies have a tendency to adjust their flying while keeping up appropriate separation in the dynamic swarm, whereas for a static swarm the dragonfly arrangement is too low when cohesion is very high which results in attack preys. Thus, it is a general tendency that for exploring and exploiting the search space, dragonflies with high alignment and low cohesion weights, and low alignment and high cohesion are used. The transition between these two states are possible by increasing the overall radius of the search space and by tuning the swarm factors during the process of optimization.

The following assumptions are made for the dragonflies so that the convergence condition can be achieved. The weight of each dragonfly has to change in the search space such that transition of exploration to exploitation is possible. Thus, during the optimization process each dragonfly tries to see some other dragonflies to alter flying way. In other word, the area region is expanded too whereby the swarm get to be one gathering at the last phase of optimization to converge, thus to converge to the global optimum. From the search space, the food source and the enemy are collected from the best and worst solutions obtained till now. Thus, a convergence condition toward the promising areas and a divergence from a non-promising areas can be achieved. Finally, the performance of artificial dragonflies can be improved by utilizing the 'Lévy flight.' According to this, if a neighboring solution is not present, then each dragonfly utilizes a random walk and flies around the search space.

Now the position of each dragonfly can be upgraded using the following expressions:

$$X_{t+1} = X_t + \text{Lévy}(d) \times X_t \tag{17}$$

where d shows the dimension of the position vectors.

The Lévy flight can be calculated as:

$$\text{Lévy}(x) = 0.01 \times \frac{r_1 \times \sigma}{|r_2|^{\frac{1}{\beta}}} \tag{18}$$

where r_1 and r_2 represent random numbers varied in the range [0, 1], β represents a constant whose value is 1.5 (in this work), σ can be calculated as:

$$\sigma = \left(\frac{\Gamma(1+\beta) \times \sin\left(\frac{\Pi\beta}{2}\right)}{\Gamma\left(\frac{1+\beta}{2}\right) \times \beta \times 2^{\left(\frac{\beta-1}{2}\right)}} \right)^{1/\beta} \quad \text{where} \quad \Gamma(x) = (x-1)$$

5.2 Pattern Search Algorithm

The pattern search (PS) algorithm is a recent developed algorithm, which can solve a number of nonlinear optimization

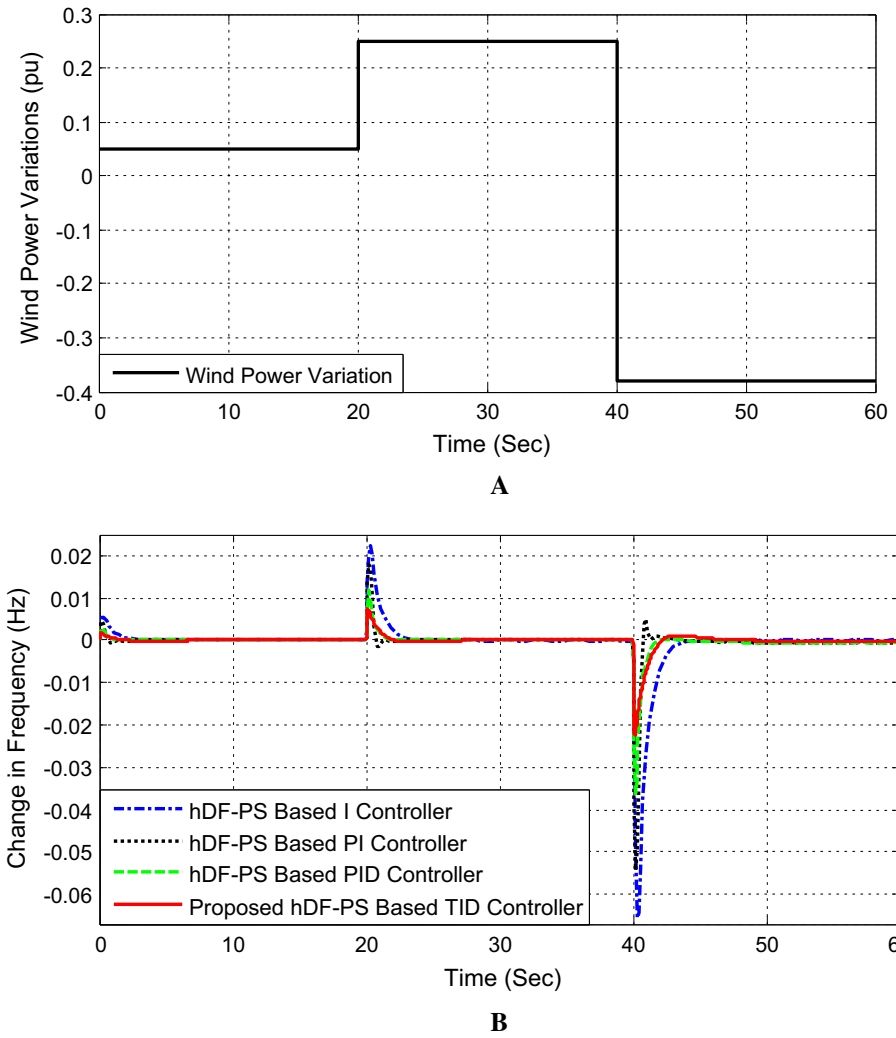

Fig. 4 **a** Wind power change pattern, **b** MG output frequency

problems. The PS algorithm is associated with numerous advantages like ease of implementation, simple concept and computationally very efficient. The operator used in the PS algorithm is well balanced and flexible and hence enhances the global search and improves the fine tune capability in the local search [27]. The PS algorithm starts with an initial point X_0 which is considered as the starting point of the algorithm. The initial point X_0 is mainly provided by the DF algorithm. Then, a pattern formation is done by adding a scalar multiple with the set of current vectors. Now it will be the current point for the next iteration if it archives a better objective function.

In the first iteration, the pattern vectors/direction vectors are constructed in the form of [0, 1], [1, 0], [−1, 0] and [0, −1]. In PS algorithm, the iteration counter is also known as mesh size. In the next step, a mesh point is created by adding the direction vectors to the initial point X_0 as $X_0 +$ [0, 1], $X_0 +$ [1, 0], $X_0 +$ [−1, 0] and $X_0 +$ [0, −1]. The objective function at all the mesh points is calculated until it reaches a smaller value than the objective function value of X_0 [28]. This point is treated as X_1 which is considered as the initial point for the next iteration. At the second iteration, the current mesh is increased by multiplying factor 2 which is also known as an expansion factor. Therefore, at the second iteration, the mesh point becomes: $X_1 + 2 \times [0, 1]$, $X_1 + 2 \times [1, 0]$, $X_1 + 2 \times [-1, 0]$ and $X_1 + 2 \times [0, -1]$, and this process is continued till the stopping criteria are achieved. If the objective function is not found to be smaller in certain iteration, then the same point will be treated as an initial point for the next iteration. In the next iteration, the initial point is multiplied by a factor 0.5 which is known as contraction factor so that the smaller objective function is obtained, and this process will be repeated till the termination condition is achieved [29]. The evaluation of objective function is done at $t = 1.0$ s by considering some disturbance.

Table 2 Comparison of different optimization techniques

Parameters	GA-based PID controller	PSO-based PID controller	DF-based PID controller	Hybrid DF–PS-based PID controller
K_p	− 1.9869	− 1.9729	− 1.8756	− 1.9898
K_i	− 0.2366	− 0.1693	− 0.1298	− 0.1371
K_d	− 1.3488	− 1.9840	− 1.8875	− 0.7208
ITAE	2.162	1.9861	1.9151	1.415

Table 3 Controller parameters for Microgrid (wind variation)

Parameters	Proposed hDF-PS-based tilt integral derivative controller	hDF-PS-based PID controller	hDF-PS-based PI controller	hDF-PS-based I controller
K_p	− 1.8988	− 1.9898	− 1.9981	–
K_i	0.0863	− 0.1371	− 0.1335	− 0.0372
K_d	− 1.9697	− 0.7208	–	–
n	5.7697	–	–	–
ITAE	1.0730	1.415	1.681	3.196

6 Simulation Results and Discussion

This section deals with the simulation results in terms of MG frequency response considering different system parameters as disturbances like ΔP_{Wind}, ΔP_{ϕ} and ΔP_{L}. The application of our proposed hybrid DF–PS algorithm on the tilt integral derivative controller is analyzed. The viability of the proposed strong methodologies is demonstrated by comparing with the optimal I, PI and PID controllers. The controller parameters are obtained using the proposed hybrid algorithm. The MG frequency response is examined by performing six disjoin test situations.

6.1 Model Verification

Here, Eq. (7) is used to find the parameters of the PID controller with an objective to minimize its fitness value. For the application of the proposed hDF-PS algorithm, the following parameters are chosen, the population size = 20, maximum iteration = 50, w is varied with in a span of 0–1. Stopping criteria are selected based on maximum iteration count.

6.2 Case-1: [Fluctuation in Wind Power (ΔP_{Wind})]

For the first instance, the step change in wind power variation (ΔP_{Wind}) is considered. Figure 4a demonstrates pattern for the variation in ΔP_{Wind}. In order to prove the effectiveness of the proposed hDF-PS algorithm, it is compared with some conventional algorithms like genetic algorithm (GA), particle swarm optimization (PSO) and dragonfly (DF) using a PID controller. Here in order to apply the GA, PSO and DF algorithms, all the initial parameters for each algorithm have been initialized. The population size is fixed to 30, and the maximum iteration is set to 50 for all individual algorithms. Table 2 shows the comparison of different algorithm by considering the above system disturbance. It can be seen from Table 2 that the performance of the hDF-PS algorithm-based PID controller provides superior result as compared to the some standard algorithms based PID controller and thus justifies the application of the above hybrid algorithm.

In the next step, the hybrid DF–PS algorithm is utilized to tune the tilt integral derivative controller by considering the same disturbance, i.e., wind power variation (ΔP_{Wind}) as shown in Fig. 4a. Table 3 shows the optimized controller parameters for the proposed hDF-PS-based multistage PID controller and also other controllers. Figure 4b illustrates the MG frequency response output showing the comparison of the proposed and the conventional controllers. As far as simulation results are concerned, the following cases are investigated:

- Case-1: The system response of the I controller with the proposed hDF-PS algorithm is represented by legend 'hDF-PS based I Controller.'
- Case-2: The response of the MG with PI controller obtained by employing the hybrid algorithm is represented by the legend 'hDF-PS based PI Controller.'
- Case-3: The PID-based MG system with the application of the hybrid algorithm is represented by the legend 'hDF-PS based PID Controller.'
- Case-4: Finally, the response of the MG with the proposed tilt integral derivative controller obtained by employing the novel hybrid DF–PS algorithm is represented by the legend 'Proposed hDF-PS based TID Controller.'

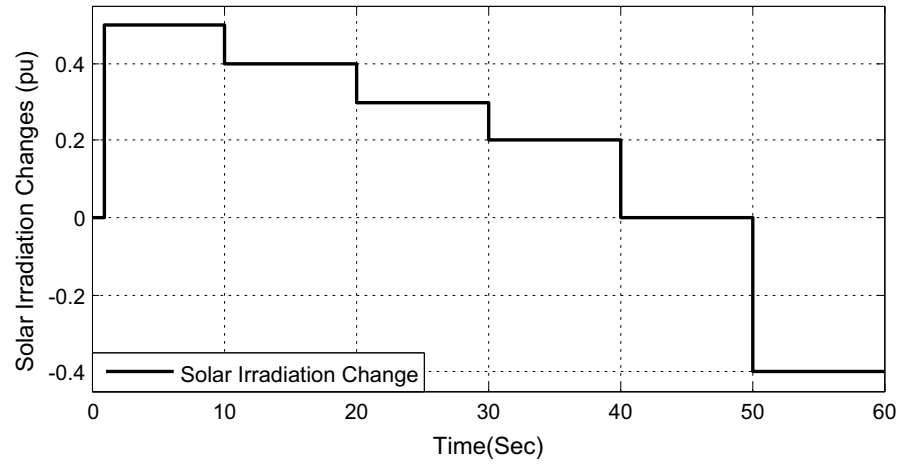

A

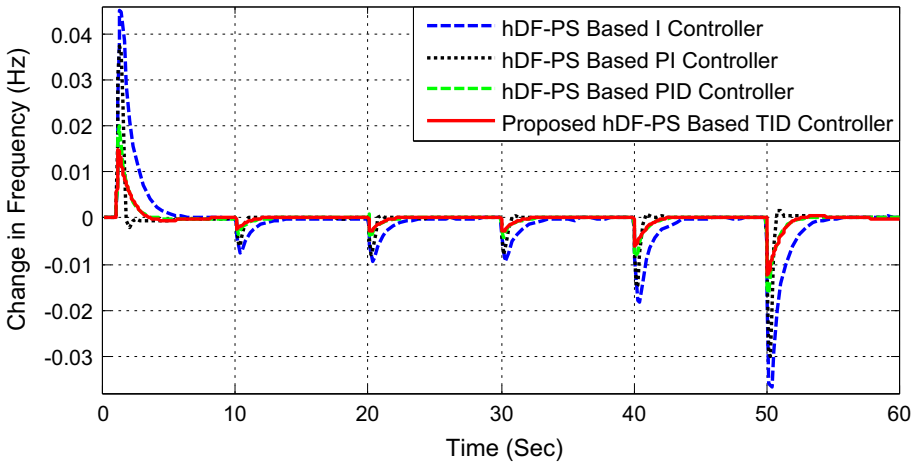

B

Fig. 5 **a** Solar power change pattern, **b** MG output frequency

Table 4 Controller parameters for Microgrid (solar irradiation variation)

Parameters	Proposed hDF-PS-based tilt integral derivative controller	hDF-PS-based PID controller	hDF-PS-based PI controller	hDF-PS-based I controller
K_p	− 1.9885	− 1.897	− 1.7898	–
K_i	− 0.1425	− 0.1425	− 0.1680	− 0.0405
K_d	− 1.1865	− 1.1865	–	–
n	5.0852	–	–	–
ITAE	1.178	1.338	1.4	3.865

It can be seen from Table 3 and Fig. 4b that the proposed TID controller along with the hDF-PS algorithm provides better results in terms of objective function and system oscillations as compared to other controllers.

6.3 Case-2: [Fluctuation in Solar Power (ΔP_ϕ)]

Simultaneously another genuine test is performed by considering a step change in sun irradiation power (ΔP_ϕ) pattern as shown in Fig. 5a. Figure 5b illustrates frequency response curve of the MG for the designed controllers. Table 4 represents the required controller parameters which are optimized using the hDF-PS algorithm for a change in solar power injection.

The same conclusion can be drawn from Table 4 that the hDF-PS-based TID controller is more stable. Simultaneously system oscillations are also damped out efficiently. It is clearly evident from Fig. 5b that the system performance improves significantly with the proposed TID controller as compared to the other controllers.

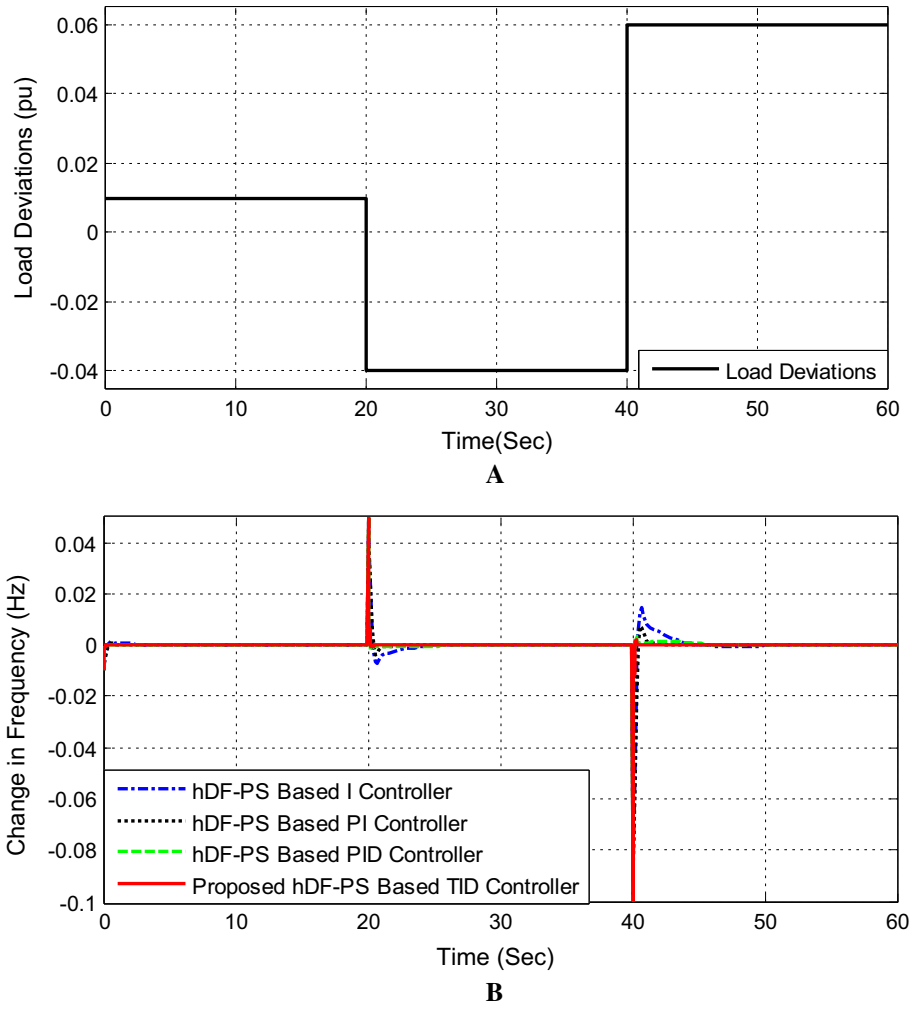

Fig. 6 **a** Multiple load variation, **b** MG output frequency

Table 5 Controller parameters for Microgrid (load variation)

Parameters	Proposed hDF-PS-based tilt integral derivative controller	hDF-PS-based PID controller	hDF-PS-based PI controller	hDF-PS-based I controller
K_p	− 0.5729	− 0.8205	0.2354	–
K_i	0.0428	− 0.804	− 0.0258	− 0.366
K_d	1.9560	− 1.9989	–	–
n	4.1112	–	–	–
ITAE	0.3967	0.658	1.297	2.119

6.4 Case-3: [Fluctuation in Load (ΔP_{Load})]

In this case, change in load deviation (ΔP_{Load}) (disturbance) is taken into account. The variation pattern is shown in Fig. 6a, b illustrating the frequency response curve of the MG through the executions of the proposed hybrid tilt integral derivative controller. The optimized controller parameters (P, PI, PID and TID) for the load disturbance are tabulated in Table 5. The same conclusion can be drawn from Fig. 6b that the hDF-PS-based TID controller yields better result in terms of system oscillations as compared to other conventional controllers.

6.5 Case-4: (Changes in ΔP_{Wind}, ΔP_{ϕ}, ΔP_{Load} and MG Parameters Simultaneously)

In this case, a simultaneous change in the different system parameters like sun irradiation, load change and the wind power is considered. Figure 7a demonstrates the change pattern for the blended changes in the disturbance parameters,

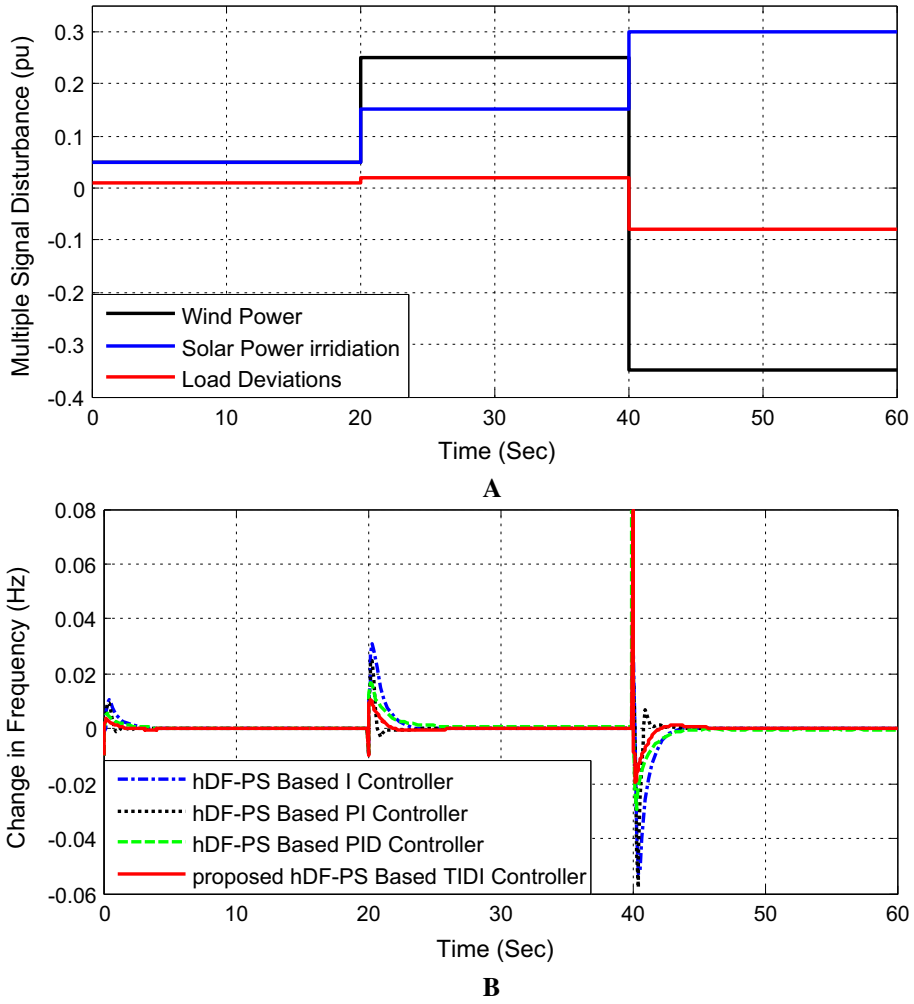

Fig. 7 **A** Multiple disturbances in load, wind speed, and solar irradiation, **b** MG output frequency

Table 6 Controller parameters for Microgrid (all variation)

Parameters	Proposed hDF-PS-based tilt integral derivative controller	hDF-PS-based PID controller	hDF-PS-based PI controller	hDF-PS-based I controller
K_p	− 1.9865	− 0.4364	− 1.9999	–
K_i	− 0.0986	− 0.0137	− 0.1333	− 0.0390
K_d	− 1.9210	− 0.9186	–	–
n	4.8583	–	–	–
ITAE	1.1230	2.4601	3.0384	7.046

and Fig. 7b demonstrates the frequency response of the MG output. Table 6 shows the controller parameters using the hybrid algorithm for a multiple change in system parameters.

From Fig. 7b, it is clearly observed that the system yields less time to regain the original system with the proposed hDF-PS-based TID controller as compared to other form of controllers like I, PI and PID controller.

7 Conclusion

In this paper, a novel approach is made by proposing a hybrid DF–PS algorithm for a tilt integral derivative controller for the frequency control of an islanded MG. The state-space model of the MG is used for the application of the control techniques. As talked about, utilizing robust controllers gives numerous advantages. As the first part of the research work, the comparison of the hybrid optimizations techniques is done with some conventional algorithm like GA, PSO and DF algorithm. These three algorithms

have been used for finding the optimal controller parameters, and it is proved that the hDF-PS provides superior result. Further the hDF-PS-based TID controllers along with the conventional controllers are planned in an approach to decrease the impacts of ΔP_{Wind}, ΔP_{ϕ} and ΔP_{Load} disturbances and dynamic perturbations. A conclusion can be made that, because of the tilted behavior of the proposed, the hDF-PS-based TID controller provides better execution over the other conventional controllers like PID, PI and I. The time-domain simulation results demonstrate that the balance in power generation and load can be effectively made by using the proposed hybrid tilt integral derivative controller; thus, the disturbances in MG frequency can be overcome.

References

1. Alzola, J.A.; Vechiu, I.; Camblong, H.; Santos, M.; Sall, M.; Sow, G.: Microgrids project, Part 2: design of an electrification kit with high content of renewable energy sources in Senegal. Renew. Energy **10**, 2151–2159 (2009)
2. Joseba, J.; Anduaga, J.; Oyarzabal, J.; Muro, A.G.: Architecture of a microgrid energy management system. Eur. Trans. Electr. Power **21**, 1142–1158 (2011)
3. Lingwei, Z.; Liu, S.; Xie, X.: Frequency domain-based configuration and power follow-up control for power sources in a grid-connected Microgrid. Int. Trans. Electr. Energy Syst. **10**, 2499–2514 (2015)
4. Guerrero, J.M.; Loh, P.C.; Lee, T.-L.; Chandorkar, M.: Advanced control architectures for intelligent microgrids—Part II: power quality, energy storage, and AC/DC microgrids. IEEE Trans. Ind. Electron. **60**, 1263–1270 (2013)
5. Nayanar, V.; Kumaresan, N.; Gounden, N.G.: Wind-driven SEIG supplying DC microgrid through a single-stage power converter. Eng. Sci. Technol. Int. J. **3**, 1600–1607 (2016)
6. Dialynas, E.; Daoutis, L.: Modelling and evaluation of microgrids reliability and operational performance and its impact on service quality. Eur. Trans. Electr. Power **21**, 1255–1270 (2011)
7. Etemadi, A.H.; Davison, E.J.; Iravani, R.: A decentralized robust control strategy for multi-DER microgrids—Part I: fundamental concepts. IEEE Trans. Power Del. **27**, 1843–1853 (2012)
8. Han, Y.; Young, P.M.; Jain, A.; Zimmerle, D.: Robust control for microgrid frequency deviation reduction with attached storage system. IEEE Trans. Smart Grid **6**, 557–565 (2015)
9. Kahrobaeian, A.; Mohamed, Y.A.I.: Direct single-loop μ-synthesis voltage control for suppression of multiple resonances in microgrids with power-factor correction capacitors. IEEE Trans. Smart Grid **4**, 1151–1161 (2013)
10. Mehrizi-Sani, A.; Iravani, R.: Potential-function based control of a microgrid in islanded and grid-connected modes. IEEE Trans. Power Syst. **25**, 1883–1891 (2010)
11. Shafiee, Q.; Guerrero, J.M.; Vasquez, J.C.: Distributed secondary control for islanded microgrid—a novel approach. IEEE Trans. Power Electron. **29**, 1018–1031 (2014)
12. Vachirasricirikul, S.; Ngamroo, I.: Robust controller design of micro-turbine and electrolyser for frequency stabilization in a microgrid system with plug-in hybrid electric vehicles. Elect. Power Energy Syst. **43**, 804–811 (2012)
13. Tan, Y.; Cao, Y.; Li, C.; Li, Y.; Yu, L.; Zhang, Z.; Tang, S.: Microgrid stochastic economic load dispatch based on two-point estimate method and improved particle swarm optimization. Int. Trans. Electr. Energy Syst. **25**, 2144–2164 (2015)
14. Bevrani, H.; Feizi, M.R.; Ataee, S.: Robust frequency control in an Islanded microgrid: H∞ and μ-synthesis approaches. IEEE Trans. Smart Grid **7**, 706–717 (2016)
15. Wu, Y.C.; Chen, M.J.; Lin, J.Y.; Chen, W.S.; Huang, W.L.: Corrective economic dispatch in a microgrid. Int. J. Numer. Model. Electron. Netw. Dev. Fields **26**, 140–150 (2013)
16. Tsikalakis, A.G.; Hatziargyriou, N.D.: Operation of microgrids with demand side bidding and continuity of supply for critical loads. Eur. Trans. Electr. Power **21**, 1238–1254 (2011)
17. Martínez, A.V.; Avila, L.I.M.; Zhang, Y.; Castañón, L.E.G.; Badihi, H.: Hybrid adaptive fault-tolerant control algorithms for voltage and frequency regulation of an islanded Microgrid. Int. Trans. Electr. Energy Syst. **25**, 827–844 (2015)
18. Sahu, R.K.; Panda, S.; Biswal, A.; Sekhar, G.C.: Design and analysis of tilt integral derivative controller with filter for load frequency control of multi-area interconnected power systems. ISA Trans. **61**, 251–264 (2016)
19. Nanda, J.; Mishra, S.; Saikia, L.C.: Maiden application of bacterial foraging based optimization technique in multi area automatic generation control. IEEE Trans. Power Syst. **24**, 602–609 (2009)
20. Ram, G.; Mandal, D.; Kar, R.; Ghoshal, S.P.: Opposition-based BAT algorithm for optimal design of circular and concentric circular arrays with improved far-field radiation characteristics. Int. J. Numer. Model. Electron. Netw. Dev. Fields **30**, 3–4 (2017)
21. Ghosal, S.P.: Optimization of PID gains by particle swarm optimization in fuzzy based automatic generation control. Electr. Power Syst. Res. **72**, 203–212 (2004)
22. Padhy, S.; Panda, S.; Mahapatra, S.: A modified GWO technique based cascade PI–PD controller for AGC of power systems in presence of plug in electric vehicles. Eng. Sci. Technol. Int. J. **20**, 427–42 (2017)
23. Khadanga, R.K.; Satapathy, J.K.: Unified power flow controller based damping controller design: a hybrid PSO–GSA approach. In: Energy, Power and Environment: Towards Sustainable Growth (ICEPE), pp. 1–6 (2015)
24. Mirjalili, S.: Dragonfly algorithm: a new meta-heuristic optimization technique for solving single objective, discrete, and multi objective problems. Neural Comput. Appl. **27**, 1053–1073 (2016)
25. Bao, Y.; Hu, Z.; Xiong, T.: A PSO and pattern search based memetic algorithm for SVMs parameters optimization. Neuro Comput. **117**, 98–106 (2013)
26. Khadanga, R.K.; Kumar, A.: Hybrid adaptive 'gbest'-guided gravitational search and pattern search algorithm for automatic generation control of multi-area power system. IET Gener. Transm. Distrib. **11**, 3257–3267 (2016)
27. Othman, A.K.; Ahmed, N.A.; AlSharidah, M.E.; Hanan, H.A.: A hybrid real coded genetic algorithm—pattern search approach for selective harmonic elimination of PWM AC/AC voltage controller. Int. J. Electr. Power Energy Syst. **44**, 123–133 (2013)
28. Bidram, A.; Davoudi, A.; Lewis, F.L.; Guerrero, J.M.: Distributed cooperative secondary control of microgrids using feedback linearization. IEEE Trans. Power Syst. **28**, 3462–3470 (2013)
29. Bevrani, H.; Habibi, F.; Babahajyani, P.; Watanabe, M.; Mitani, Y.: Intelligent frequency control in an AC microgrid, Online PSO-based fuzzy tuning approach. IEEE Trans. Smart Grid **4**, 1935–44 (2012)